

## Three-Dimensional Phase-Only Holographic Correlation

Taegeun Kim\*

*Department of Optical Engineering, Sejong University, Seoul 143-747, KOREA*

(Received June 5, 2001)

This paper presents a phase-only modulation scheme for a three-dimensional (3-D) image matching system to improve optical efficiency of the system. The 3-D image matching system is based on the two mask heterodyne scanning. A hologram of the 3-D reference object is first created and then the phase of the hologram is extracted. The phase of the hologram is represented as one mask with the other mask being a plane wave. The superposition of each beam modulated by the two masks generates a scanning beam pattern. This beam pattern scans the 3-D target object to be recognized. The output of the scanning system gives out the correlation of the phase-only hologram of the reference object and the complex hologram of the target object. Since a hologram contains 3-D information of an object as a form of fringe pattern, the correlation of holograms matches whole 3-D aspect of the objects. Computer simulations are performed with additive gaussian noise and without noise for the complex hologram modulation scheme and the phase-only hologram modulation scheme. The computer simulation results show that the phase-only hologram modulation scheme improves the optical efficiency. Thus the system with the phase-only hologram modulation scheme is more robust than the system with the complex hologram modulation scheme.

*OCIS codes* : 070.4550, 070.5010, 090.0090, 100.5090, 100.6890.

### I. INTRODUCTION

The main objective of this paper is to investigate a three dimensional (3-D) holographic correlation technique with a phase-only mask. 3-D correlation has been one of the most challenging problems in the pattern recognition area, largely due to attempts to endow pattern recognition systems with robust visual capabilities and a variety of applications [1]. The real spatial world is 3-D. Thus 3-D information of objects can give a pattern recognition system more robust visual capabilities. 3-D correlation is a formidable task, mainly due to visual systems that are restricted to the sensing and processing of information that can be displayed as 2-D projections [1]. For a higher order correlation operation, trans-dimensional mapping and matching the dimension-reduced signals has been proposed [2]. Especially for 3-D correlation, 3-D to 2-D planar encoding and matching was proposed [3]. However, these two proposed techniques are restricted to 3-D correlation of the given 3-D information of objects, and require a lot of 2-D sampling images for high resolution performance. In 3-D image recognition, the extraction of 3-D information about objects is another critical issue because conventional imaging systems are restricted to two dimensions. An inter-

esting idea for 3-D correlation has been proposed, in which 3-D information about an object is extracted by moving a CCD camera transversely. The 3-D information is processed by 2-D optical Fourier transformations. However, this proposed technique also requires many 2-D images and a 3-D discrete Fourier transformation [4].

Most recently, the use of holographic information to represent 3-D objects for optical 3-D object recognition was proposed and studied [5-9]. It has been shown that, by using optical scanning holography, one can achieve optical recognition of 3-D objects by 2-D correlation between the holograms of the 3-D reference object and 3-D target objects. It is important to point out that the 2-D correlation of the holograms can match the 3-D aspect of the 3-D objects because the hologram has depth information about the 3-D object as a form of 2-D fringe pattern, as well as transverse information about the 3-D object. In the proposed technique, a hologram of the 3-D reference object is first created and then represented as one mask with the other mask being a plane wave. The superposition of each beam modulated by the two masks generates a scanning beam pattern. This beam pattern scans the 3-D target object to be recognized. The output of the scanning system gives out the 2-D correlation of

the hologram of the reference object and that of the target object. When the 3-D image of the target object is matched with that of the reference object, the output of the system generates a strong correlation peak. In the proposed technique the scanning beam is modulated spatially by the complex hologram. This modulation scheme suffers from a low power correlation signal. Because the complex hologram blocks most light by amplitude, the intensity of the modulated scanning beam is small, and this generates a weak correlation signal against the system noise. If the correlation signal is small, compared to the noise level of the system, it is undetectable. Even though this can be overcome by increasing the intensity of the laser, the size and the power of the laser are limited in a real situation. Thus, increasing the power of the correlation signal with a given power of the laser is necessary to improve the robustness of the system.

In this paper, we propose a phase-only mask as a modulation scheme to improve the robustness of the system. The phase-only matched filtering technique was proposed to increase the optical efficiency of the conventional 2-D optical correlators [10,11]. The idea of the phase-only matched filtering technique originated from the fact that the phase information of the image in the frequency domain plays an important role in preserving the visual intelligibility of the image, compared to the intensity information of the image in the frequency domain [12]. In addition, a phase-only filter does not consume the power of the light because a phase-only object does not block the light, but merely changes the direction of the beam.

In section 2, we review the 3-D holographic correlation technique and shows the 3-D matching capabilities of the proposed technique. In section 3, we propose the phase-only modulation scheme to improve optical efficiency of the 3-D holographic correlation

technique. The section 4 presents the computer simulation results that compare the discrimination ability and the optical efficiency between the complex hologram modulation scheme and phase-only modulation scheme. The computer simulations are performed with additional gaussian noise and without noise. The computer simulation results show the robustness of the proposed modulation scheme against the additional gaussian noise.

## II. THREE-DIMENSIONAL HOLOGRAPHIC CORRELATION

A rigorous mathematical analysis of the three-dimensional holographic correlation technique based on the spatial-frequency domain analysis has already been described [5]. Thus in this section, we present a brief and intuitive description of the system. Fig. 1 shows the optical heterodyne scanning system. In Fig. 1, the laser beam generated by HeNe laser is split into two paths by a beam splitter. The temporal frequency of each beam is shifted by an acousto-optic frequency shifter, operating at frequency  $\Omega$ . These beams are collimated by beam expanders BE1 and BE2. Each collimated beam is modulated spatially by masks,  $m_1$  and  $m_2$  respectively, and are combined by a beam splitter, BS1. The intensity pattern of the combined beam,  $I_s(x, y; z)$  at a distance  $z$  away from the masks is given by

$$I_s(x, y; z) = |m_{1z}(x, y) \exp[j(\omega_o + \Omega)t] + m_{2z}(x, y) \exp(j\omega_o t)|^2, \quad (1)$$

where  $m_{1z}(x, y)$  and  $m_{2z}(x, y)$  are respectively diffracted patterns of masks  $m_1(x, y)$  and  $m_2(x, y)$ , that are given by

$$m_{iz}(x, y) = m_i(x, y) \otimes h(x, y; z); i = 1, 2, \quad (2)$$

where  $h(x, y; z)$  is called the free space impulse response, and is given by

$$h(x, y; z) = \frac{jk_o}{2\pi z} \exp\left[-j\frac{k_o}{2z}(x^2 + y^2)\right], \quad (3)$$

with  $k_o$  representing the wave number of the scanning beam and  $\otimes$  denoting the 2-D convolution operation, which is defined as:

$$g_1(x, y) \otimes g_2(x, y) = \int \int g_1(x', y') g_2(x - x', y - y') dx' dy'. \quad (4)$$

When the 3-D intensity pattern of the combined beam,  $I_s(x, y; z)$  scans on the  $I_o(x, y; z)$  object amplitude transparency, located  $z$  away from the masks as

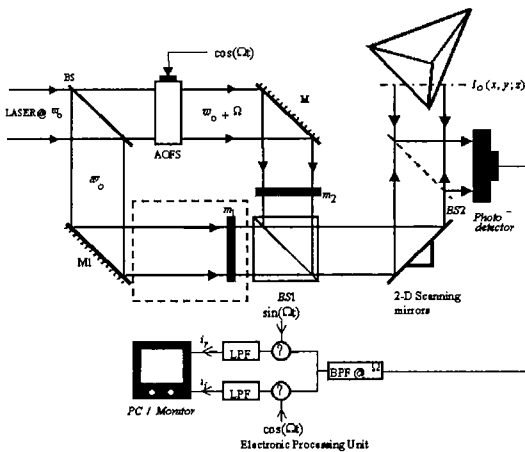


FIG. 1. Optical scanning holography system (BS, BS1, BS2: beam splitters, M, M1: mirrors,  $m_1, m_2$ : masks, AOFS: acousto-optic frequency shifter; BPF@ $\Omega$ : band pass filter tuned at frequency  $\Omega$ ; LPF: low pass filter).

shown in Fig. 1, the total intensity passes through  $I_o(x, y; z)$  is given by

$$\begin{aligned} I(x, y) &= \iint I_s(x', y'; z) I_o(x + x', y + y'; z) dx' dy', \\ &= I_s(x, y; z) \odot I_o(x, y; z). \end{aligned} \quad (5)$$

Note that the total intensity that passes through the object intensity transparency is proportional to the correlation between the scanning beam and the object amplitude transparency. The symbol  $\odot$  in Eq. (5), denotes the 2-D correlation operation that is defined as:

$$Re\{m_{1z}(x', y') m_{2z}^*(x', y')\} \odot I_o(x, y; z), \text{ and } Im\{m_{1z}(x', y') m_{2z}^*(x', y')\} \odot I_o(x, y; z), \quad (7)$$

where  $Re\{\cdot\}$  and  $Im\{\cdot\}$  represent the real part of and the imaginary part of the cross term of the scanning beam respectively.

Note that the undesirable space-variant DC terms have been eliminated due to the heterodyne photo detection. The two outputs respectively represent the correlation between the real part of, and the imaginary part of the product of the diffraction patterns of each mask, and the object intensity. For a general 3-D object that is distributed along  $z$  as well as  $x - y$  distribution, Eq. (7) are integrated along the depth  $z$  due to the superposition. These are given by

$$i_r(x, y) = \int Re\{m_{1z}(x, y) m_{2z}^*(x, y) \odot I_o(x, y; z)\} dz, \quad (8)$$

$$i_i(x, y) = \int Im\{m_{1z}(x, y) m_{2z}^*(x, y) \odot I_o(x, y; z)\} dz. \quad (9)$$

### 1. Recording stage of the holographic information of objects

Fig. 1 shows the optical system in the recording stage of holographic information of an object. Here, we choose masks,  $m_1(x, y) = \delta(x, y)$  and  $m_2(x, y) = 1$  then scan a reference object,  $R(x, y; z)$  i.e., we let  $I_o(x, y; z) = R(x, y; z)$ . The diffracted pattern from the first mask,  $m_1(x, y) = \delta(x, y)$  is the spherical wave,  $m_{1z}(x, y) = (jk_o/2\pi z) \exp[-j\{(x^2 + y^2)k_o/2z\}]$  and the diffracted pattern from the second mask,  $m_2(x, y) = 1$ , is the plane wave,  $m_{2z}(x, y) = 1$ . Thus, 3-D distribution of the scanning beam pattern is the Fresnel zone pattern. That is given by

$$\begin{aligned} g(x, y) \odot h(x, y) \\ = \iint g^*(x', y') h(x + x', y + y') dx' dy'. \end{aligned} \quad (6)$$

The total intensity is collected and transformed to an electric signal by the photo-detector. The current output that is proportional to the total intensity consists of a DC term and heterodyne term with temporal frequency at  $\Omega$ .

The in-phase and the quadrature-phase components of the heterodyne term of the output current are extracted by respectively multiplying it with  $\sin(\Omega t)$ ,  $\cos(\Omega t)$  and low-pass filtering. These are given by

$$m_{1z}(x, y) m_{2z}^*(x, y) = \frac{jk_o}{2\pi z} \exp\left[-j \frac{(x^2 + y^2)k_o}{2z}\right]. \quad (10)$$

One output of the system is the correlation between the real part of the Fresnel zone pattern and the intensity distribution of the object, that corresponds to the cosine hologram of the object as in Eq. (8). The other output of the system is the correlation between the imaginary part of the Fresnel zone pattern and the intensity distribution of the object, that corresponds to the sine hologram of the object as in Eq. (9). Thus, the outputs of the system are cosine and sine holograms of the reference object. These are given by

$$i_r(x, y) = \int \frac{k_o}{2\pi z} \cos\left[\frac{k_o}{2z}(x^2 + y^2)\right] \odot R(x, y; z) dz, \quad (11)$$

$$i_i(x, y) = \int \frac{k_o}{2\pi z} \sin\left[\frac{k_o}{2z}(x^2 + y^2)\right] \odot R(x, y; z) dz. \quad (12)$$

These output currents of the system are stored in a digital computer using an analog-to-digital converter. In the digital computer, the complex hologram is achieved by adding two holograms in a complex manner:

$$\begin{aligned} H_R(x, y) &= i_r(x, y; z) + j i_i(x, y; z) \\ &= \int j \frac{k_o}{2\pi z} \exp\left[\frac{-jk_o}{2z}(x^2 + y^2)\right] \\ &\quad \odot R(x, y; z) dz, \end{aligned} \quad (13)$$

Note that the complex hologram of an object has the depth information of the object as a form of fringe pattern.

## 2. 3-D image matching stage

After the complex hologram of the object is recorded as described in sub-section 2.1, the object is removed. We shall call the hologram as a reference hologram as the object being recorded is the reference object. The reference hologram will be used to match a 3-D target.

In the matching stage, a target object,  $T(x, y; z)$

now is placed  $z$  away from the masks of the scanning system. Let  $m_1(x, y) = H_R(x, y)$ , and keep  $m_2(x, y) = 1$  as in the holographic recording stage and then the target object,  $T(x, y; z)$  is scanned by the system.

The diffracted pattern from the first mask,  $m_1(x, y) = H_R(x, y)$ , is the reconstructed image of the reference hologram. That is given by

$$m_{1z}(x, y) = \left\{ \int \frac{jk_o}{2\pi z} \exp \left[ \frac{-jk_o}{2z} (x^2 + y^2) \right] \odot R(x, y; z) dz \right\} \otimes h(x, y; z). \quad (14)$$

The diffracted pattern from the second mask,  $m_2(x, y) = 1$ , is the plane wave,  $m_{2z}(x, y) = 1$ . Thus, 3-D distribution of the scanning beam is the reconstructed image of the reference hologram. That is given by

$$m_{1z}(x, y) m_{2z}^*(x, y) = \left\{ \int \frac{jk_o}{2\pi z} \exp \left[ \frac{-jk_o}{2z} (x^2 + y^2) \right] \odot R(x, y; z) dz \right\} \otimes h(x, y; z). \quad (15)$$

Note that the 3-D distribution of the scanning beam is the same as the actual intensity distribution of the reference object.

According to Eqs. (8) and (9), the output currents are given by

$$\begin{aligned} i_r(x, y; z) &= Re [m_{1z}(x, y) m_{2z}^*(x, y)] \odot T(x, y; z), \\ &= Re \left[ H_R(x, y) \otimes H(x, y; z) \right] \odot T(x, y; z), \\ &= Re \left[ \left\{ \int \frac{jk_o}{2\pi z} \exp \left[ \frac{-jk_o}{2z} (x^2 + y^2) \right] \odot R(x, y; z) dz \right\} \otimes h(x, y; z) \right] \odot T(x, y; z), \\ &= Re \left[ \left\{ \int \frac{jk_o}{2\pi z} \exp \left[ \frac{-jk_o}{2z} (x^2 + y^2) \right] \odot R(x, y; z) dz \right\} \right. \\ &\quad \left. \odot \left\{ \int \frac{jk_o}{2\pi z} \exp \left[ \frac{-jk_o}{2z} (x^2 + y^2) \right] \odot T(x, y; z) dz \right\} \right], \\ &= Re \left[ H_R(x, y) \odot H_T(x, y) \right], \end{aligned} \quad (16)$$

where  $H_T(x, y)$  is the complex hologram of the target object,  $T(x, y)$ .

Eq. (16) demonstrates that the system can perform correlation of two holographic information, and hence 3-D image matching is possible.

## III. PHASE-ONLY HOLOGRAM MODULATION SCHEME

The proposed 3-D holographic correlation technique in section 2 suffers from a low power correlation signal. Because the complex hologram blocks most light by amplitude, the intensity of the modulated scanning beam is small, and this generates a weak correlation signal against the system noise. If the correlation signal is small, compared to the noise level of the system,

it is undetectable. Even though this can be overcome by increasing the intensity of the laser, the size and the power of the laser are limited in a real situation. Thus, increasing the power of the correlation signal with a given power of the laser is necessary to improve the robustness of the system.

### 1. Optical efficiency

Optical efficiency is a critical issue for the 3-D holographic correlation because the robustness of the 3-D holographic matching system about the noise of the system highly depends on the optical efficiency. The optical efficiency, or Horner efficiency means the ratio of the energy in correlation to the total energy of the input signal. That is defined as [9,10]:

$$\eta_H = \eta_M \frac{\int \int |f(x, y) \otimes g^*(x, y)|^2 dx dy}{\int \int |f(x, y)|^2 dx dy}. \quad (17)$$

where  $f(x, y)$  is any input function,  $g(x, y)$  is a reference function, and  $\eta_M$  is the medium's efficiency.

In the 3-D holographic matching system, the hologram of the reference object and the hologram of the target object are the reference function and the target function, respectively.

Because the 3-D holographic image matching system uses the complex hologram of the reference object as one mask, most of the light is blocked by the amplitude of the hologram. Thus, the optical efficiency of the 3-D holographic matching system is insufficient.

The phase-only matched filtering technique was proposed to increase the optical efficiency of the conventional 2-D optical correlators [10,11]. The idea of the phase-only matched filtering technique originated from the fact that the phase information of the image in the frequency domain plays an important role in

preserving the visual intelligibility of the image, compared to the intensity information of the image in the frequency domain [12]. In addition, a phase-only filter does not consume the power of the light because a phase-only object does not block the light, but merely changes the direction of the beam.

## 2. Phase-only hologram

This sub-section introduces the phase-only hologram, in which the 3-D information of a 3-D object is preserved because both the depth information and the transverse information of a 3-D object are contained in the phase term of a hologram.

The complex hologram of the reference object in the frequency domain is achieved by the Fourier transformation of the complex hologram which is achieved in the recording stage:

$$\begin{aligned} F\{H_R(x, y)\} &= F\left\{ \int j \frac{k_o}{2\pi z} \exp\left[\frac{-jk_o}{2z}(x^2 + y^2)\right] \odot R(x, y; z) dz \right\} \\ &= \int \left[ F^* \left\{ j \frac{k_o}{2\pi z} \exp\left[\frac{-jk_o}{2z}(x^2 + y^2)\right] \right\} \times F\{R(x, y; z)\} \right] dz \\ &= \int \left[ \exp\left\{ j \frac{z}{2k_o}(k_x^2 + k_y^2) \right\} F\{R(x, y; z)\} \right] dz, \end{aligned} \quad (18)$$

where  $F\{\cdot\}$  denotes the Fourier transform operation and is defined as  $F\{u(x, y)\}_{k_x, k_y} = \int \int u(x, y) \exp(jk_x x + jk_y y) dx dy = U(k_x, k_y)$  with  $k_x$  and  $k_y$  denoting the spatial frequencies, and with the upper case function  $U$  denoting the transform of the lower case function  $u$ .

Note that the Fourier transformation of an image is in general complex with  $F\{R(x, y; z)\}$  being represented as:

$$F\{R(x, y; z)\} = A(k_x, k_y; z) \exp(j\Phi(k_x, k_y; z)). \quad (19)$$

The phase,  $\Phi(k_x, k_y; z)$  is far more significant than its intensity,  $A(k_x, k_y; z)$ . In general, the phase information contains the locations of objects in them [12]. In particular, the information of the shifted location of an object is contained only in the phase by adding a linear phase term.

Thus, the hologram in frequency domain is expressed using the amplitude and phase parts of images with additional phase terms of the free space impulse response function, that is given by:

$$\begin{aligned} F\{H_R(x, y)\} &= \int \left[ A(k_x, k_y; z) \exp(j\Phi(k_x, k_y; z)) \exp\left\{ j \frac{z}{2k_o}(k_x^2 + k_y^2) \right\} \right] dz \\ &= \int \left[ A(k_x, k_y; z) \exp\left\{ j \left[ \Phi(k_x, k_y; z) + \frac{z}{2k_o}(k_x^2 + k_y^2) \right] \right\} \right] dz. \end{aligned} \quad (20)$$

Note that the depth information of a 3-D object is contained in the phase of the hologram. Thus, the phase of the hologram in the frequency domain has both depth information and transverse information of

the 3-D object.

We define a phase-only hologram in the frequency domain to be

$$F\{H_R(x, y)\}_\Phi = \exp[j\arg(F\{H_R\})], \quad (21)$$

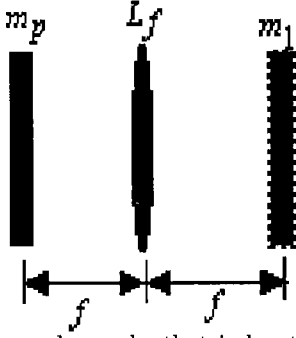


FIG. 2. Phase-only masks that is located at the back focal point of the lens  $L_f$ .

where  $\arg\{\cdot\}$  represents the argument operation of complex number.

Note that the phase-only hologram is composed of the unit amplitude and phase of the complex hologram in frequency domain. Because the spectral magnitude of an image tends to drop off at high frequencies, the phase-only image is the high frequency enhanced version of the image. In it, lines, edges and other narrow events are emphasized without modifying their position [12]. Especially in the hologram, the holographic information is contained in the high frequencies of phase as a form of chirp type signal, as shown in Eq.(20). Thus, in the phase-only hologram, the whole 3-D lines, edges and other narrow events are emphasized, and the matching accentuated narrow events will give better discrimination ability.

### 3. 3-D image matching system with a phase-only hologram

In the phase-only 3-D holographic image matching system, the phase-only hologram of the reference object in the frequency domain is place at the Frequency plane, instead of the complex hologram. This increases the optical efficiency and sensitivity of the system.

This section discusses the correlation between the phase-only hologram of the reference object and the complex hologram of the target object with high optical efficiency. We introduce a Fourier transform lens

$L_f$  with focal length  $f$  and a phase-only mask  $m_p$  in the Frequency domain, that are shown in the Fig. 2. The lens and the phase-only mask shown in the Fig. 2 is located at the place of the mask of the Fig. 1 instead of mask  $m_1$ . We set the makes,  $m_2 = 1$  and the phase-only mask,  $m_p$  equals the phase-only hologram in the Frequency domain, that is given by

$$m_p(x, y) = \exp[j\arg(F\{H_R\})]_{k_x=k_0x/f, k_y=k_0y/f}. \quad (22)$$

Note that the spatial distribution of light at the location of mask  $m_1$  equals the inverse Fourier transform of phase-only hologram of the reference object in the frequency domain, that is given by

$$m_1(x, y) = F^{-1}\{\exp[j\arg(F\{H_R\})]\}. \quad (23)$$

Note that spatial distribution of light is modulated by masks that are composed only of phase. Thus, 100 % of the light passes through the system, scans the target object. This gives high optical efficiency to the system which makes the system very robust about the noise.

The diffracted pattern from the spatial distribution of light at the location of mask  $m_1(x, y) = F^{-1}\{\exp[j\arg(F\{H_R\})]\}$  is the reconstructed image of the phase-only hologram. That is given by

$$m_{1z}(x, y) = \{F^{-1}\{\exp[j\arg(F\{H_R\})]\} \otimes h(x, y; z). \quad (24)$$

The diffracted pattern from the second mask,  $m_2(x, y) = 1$ , is the plane wave,  $m_{2z}(x, y) = 1$ . Thus, 3-D distribution of the scanning beam is the reconstructed image of the phase-only hologram. That is given by

$$m_{1z}(x, y)m_{2z}^*(x, y) = \{F^{-1}\{\exp[j\arg(F\{H_R\})]\} \otimes h(x, y; z). \quad (25)$$

Note that the 3-D distribution of the scanning beam is the high frequency emphasized version of the reference object. According to Eq. (8), the output current are given by

$$\begin{aligned} i_r(x, y; z) &= \text{Re}[m_{1z}(x, y)m_{2z}^*(x, y)] \odot T(x, y; z), \\ &= \text{Re}\{\{F^{-1}\{\exp[j\arg(\Im\{H_R\})]\}\} \odot H_T(x, y)\} \\ &= \text{Re}[H_{PR} \odot H_T(x, y)], \end{aligned} \quad (26)$$

where  $H_{PR}(x, y) = F^{-1}\{\exp[j\arg(F\{H_R\})]\}$  and  $H_T(x, y) = \int h(x, y; z) \odot T(x, y; z) dz$ .

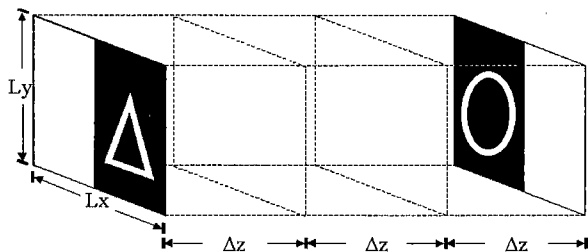
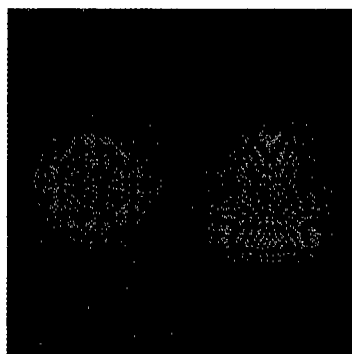
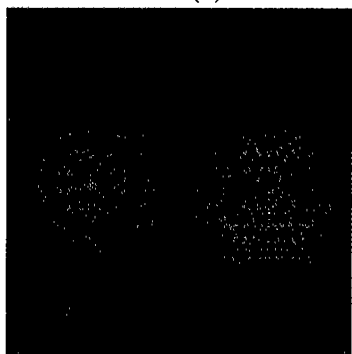


FIG. 3. 3-D reference object  $R$ , with  $L_x = L_y = 1$  cm,  $\Delta z = 1$  cm.



(a)



(b)

FIG. 4. (a) Cosine-FZP hologram of 3-D reference object. (the scanned area is  $1\text{ cm} \times 1\text{ cm}$ ) (b) Sine-FZP hologram of 3-D reference object. (the scanned area is  $1\text{ cm} \times 1\text{ cm}$ )

The  $i_r(x, y)$  given in Eq. (26) is the display of a 2-D pattern which basically represents the correlation between the phase-only hologram of the reference object and the complex hologram of the target object. It is shown that the correlation between the phase-only reference image and the target image gives the sharp correlation peak compared to the conventional corre-

lation, with high robustness [10]. The robustness of the system is a critical issue in practical realization. The previous section showed that the system with a phase-only hologram as a mask provides 100 % optical efficiency. It is obvious that this gives the strong signal compared to the complex hologram case. This makes the system with the phase-only hologram more robust to system noise that is attributed to the detector and optical components of the system itself [10]. Besides of this factor, section 4 considers the robustness of the proposed system against noise that is in the original input image, by means of computer simulations.

#### IV. COMPUTER SIMULATIONS

For matched cases and mis-matched cases, 3-D image matching tests are performed with noise added, and without noise. Noise is added to the image of the target object, but not the holograms of the reference object, which are used to spatially modulate the scanning beam. Additive intensity noise is the intensity of a Gaussian noise having a zero mean and a standard deviation  $\sigma$ . The signal to noise ratio (SNR) that is related to Gaussian noise having standard deviation,  $\sigma$ , is given by  $\text{SNR}=1/\sigma$  [9]. Additive Gaussian noise is generated by a random number subroutine in the computer. Fig. 3 shows a  $1\text{ cm} \times 1\text{ cm} \times 3\text{ cm}$  3-D reference object,  $R$ , consisting of a “triangle” and a “circle,” separated by 3 cm along the depth of the object. Figs. 4(a) and (b) plot the cosine-FZP hologram and the sine-FZP hologram of the reference object,  $R$ , as calculated by Eqs. (11) and (12), with  $z=26$  cm for the “triangle” and 29 cm for the “circle” of the 3-D reference object. The wavelength of light that is used, is  $0.6\ \mu\text{m}$  for  $h$ . The scanned area of the hologram is  $1\text{ cm} \times 1\text{ cm}$ . Physically, these holograms would correspond to the scanning of  $R$ , with its front face located 26 cm away from the scanning mirrors. Again, the masks have been chosen such that  $m_1(x, y) = 1$  and  $m_2(x, y) = \delta(x, y)$  for holographic recording, as described in the section (2.1).

For the test of the system which uses the complex hologram as a mask, the complex hologram of the reference object is generated by adding holograms as shown in figs. 4(a) and (b). Then, this is used to modulate the scanning beam. Six separate matching tests are performed for the complex hologram case, both with and without noise.

First, the target object that has the same 3-D image of the reference object is chosen for the test of the matched case without noise. Holograms of the target object are the same as those of the reference object.

TABLE 1. Matching results for noise-free inputs (Peak height is normalized to the height of the auto-correlation peak in the absence of noise.  $\Delta(\%)$  is the percentage difference between the peak heights of auto-correlations and those of cross-correlations.  $\eta_H(\%)$  is the Horner efficiency)

Noiseless Case				
Modulation scheme	Target objet	Peak height	$\Delta(\%)$	$\eta_H(\%)$
Complex Hologram	Mached Obj. (Fig.3)	1		5.91
Complex Hologram	Longitudinally Mis-matched Obj. (Fig.6)	0.0152	98	3.05
Phase-Only Hologram	Transversely Mis-matched Obj. (Fig.7)	0.7088	29	5.96
Phase-Only Hologram	Matched Obj. (Fig.3)	223		100
Phase-Only Hologram	Longitudinally Mis-matched Obj. (Fig.6)	20.87	91	100
Phase-Only Hologram	Transversely Mis-matched Obj. (Fig7)	164.45	26	100

TABLE 2. Matching results for inputs with additive noise (Peak height is normalized to the height of the auto-correlation peak in the absence of noise.  $\Delta(\%)$  is the percentage difference between the peak heights of auto-correlations and those of cross-correlations.  $\eta_H(\%)$  is the Horner efficiency)

Gaussian noise with zero mean and standard deviation, $\sigma=0.25$				
Modulation scheme	Target objet	Peak height	$\Delta(\%)$	$\eta_H(\%)$
Complex Hologram	Mached Obj. (Fig.3)	1.2825		1.72
Complex Hologram	Longitudinally Mis-matched Obj. (Fig.6)	0.0283	98	1.94
Phase-Only Hologram	Transversely Mis-matched Obj. (Fig.7)	0.9363	27	1.72
Phase-Only Hologram	Matched Obj. (Fig.3)	226.29		100
Phase-Only Hologram	Longitudinally Mis-matched Obj. (Fig.6)	22.22	90	100
Phase-Only Hologram	Transversely Mis-matched Obj. (Fig.7)	171.59	24	100

Thus, the system gives out the strong correlation peak according to Eq. (16). The intensity pattern of the system output,  $|i_s + j i_c|^2$  shown in Fig. 5. The peak height and optical efficiency are calculated according to Eqs. (16) and (17) respectively, and shown in Table I.

Second, for the test of the longitudinally mis-matched case without noise, the target object which is composed of the same 2-D patterns as those in the reference object, but located at different depths as shown

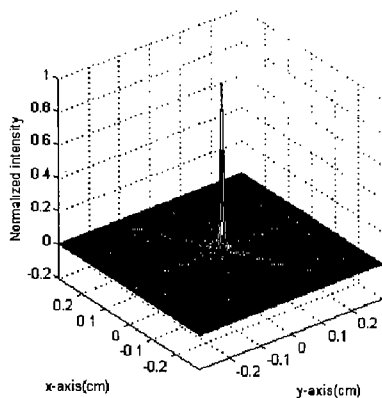


FIG. 5. Correlation output ( $0.4 \text{ cm} \times 0.4 \text{ cm}$ ) when the target object is matched with the reference object.

in Fig. 6, is chosen. The peak height and optical efficiency are calculated according to Eqs. (16) and (17) respectively, and shown in Table II. The peak height of the longitudinally mis-matched case is lower than that of the matched case because the fringe pattern of the hologram of the target object is not matched with that of the reference object. In order to have a strong correlation peak, the 3-D object have to be matched precisely throughout the whole 3-D volume.

Third, for the test of the transversely mis-matched case without noise, the target object whose 2-D slides are slightly different from those of the reference object, but located at the same depth as the reference object. The peak height and optical efficiency are calculated according to Eqs. (16) and (17) respectively, and shown in Table I. The peak height of the trans-

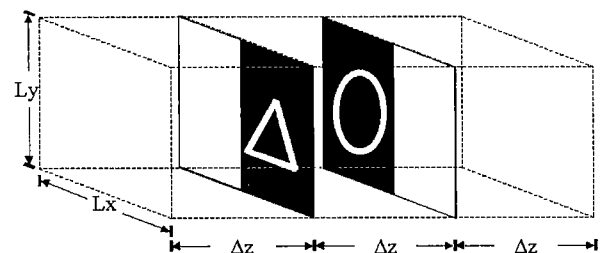


FIG. 6. 3-D target object  $T$ .



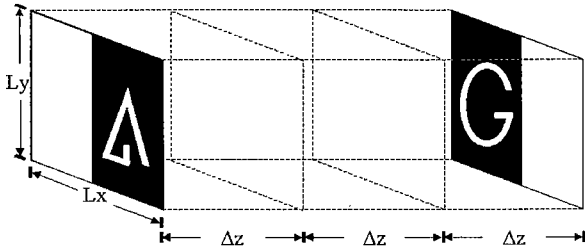
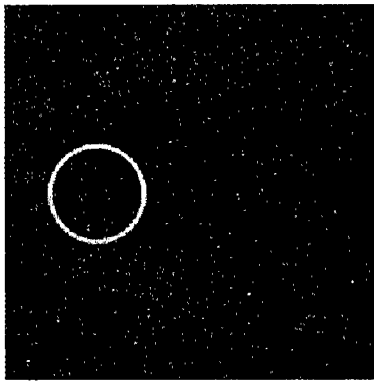


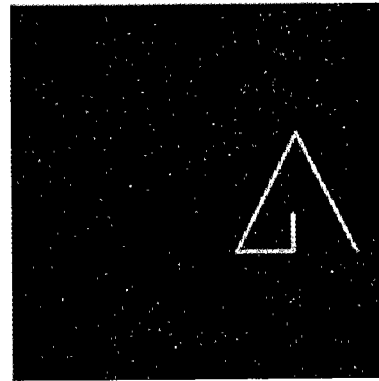
FIG. 7. 3-D target object  $T$ .



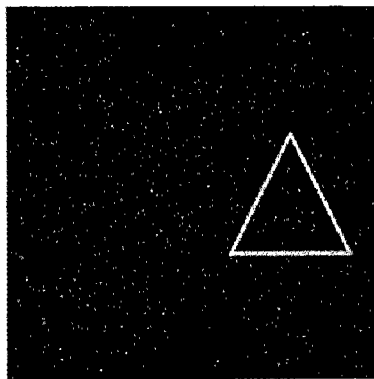
(a)



(a)



(b)



(b)

FIG. 8. (a) The first slide that composes the target object with Gaussian noise having standard deviation,  $\sigma=0.25$ . (b) The second slide that composes the target object with Gaussian noise having standard deviation,  $\sigma=0.25$ .

object is shown in Fig. 7. In order to compare discrimination ability between proposed two different modulation schemes, we choose the slides whose spatial distribution is slightly different from that of the reference

FIG. 9. (a) The first slide that composes the target object with Gaussian noise having standard deviation,  $\sigma=0.25$ . (b): The second slide that composes the target object with Gaussian noise having standard deviation,  $\sigma=0.25$ .

versely mis-matched case is also lower than that of matched case because the 2-D pattern of the target object is not matched with that of the reference object.

Fourth, for the test of the matched case in the presence of noise, the intensity of Gaussian noise with standard deviation,  $\sigma=0.25$  is added to the same target object that is used in the first case. Images of each slide with noise are shown in Figs. 8(a) and (b). The peak height and optical efficiency are calculated according to Eqs. (16) and (17) respectively, and are shown in table (2).

Fifth, for the longitudinally mis-matched case in the presence of noise, the intensity of Gaussian noise with standard deviation,  $\sigma=0.25$  is added to the same target object that is used in the second case as shown in Fig. 6. The peak height and optical efficiency are calculated according to Eqs. (16) and (17) respectively, and are shown in Table II.

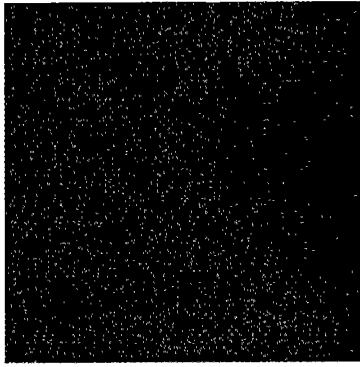


FIG. 10. Phase-only hologram of the 3-D reference object shown in Fig. 3.

Sixth, for the transversely mis-matched case in the presence of noise, the intensity of Gaussian noise with standard deviation  $\sigma=0.25$  is added to the same target object that is used in the third case as shown in Fig. 7. Images of each slide with noise are shown in Figs. 9(a) and (b). The peak height and optical efficiency are calculated according to Eqs. (16) and (17) respectively, and are shown in Table II.

For the test of the system which uses the phase-only hologram as a mask, the same tests in the complex hologram case are repeated. In these tests, the phase-only hologram of the reference object is used to modulate spatial distribution of the scanning beam. Fig. 10 represents the phase-only hologram in the Frequency domain as a gray level -black denotes zero radian and white denote  $2\pi$  radian. Fig. 11 shows respectively the intensity outputs of the system for the matched case in the absence of noise. The same tests of the system are performed in the presence of noise. For each tests with phase-only hologram modulation scheme, the peak-heights and optical efficiencies are calculated according to Eqs. (16) and (17) respectively. Tables I and II show the peak heights of system outputs and optical efficiencies for both spatial modulation schemes in the absence of noise and in the presence of noise respectively. In the Tables I and II, we can see that there is very little difference between the proposed two spatial modulation schemes, except that the peak height of the phase-only spatial modulation scheme is much larger than that of the others. When the output's peak height of the matched case with complex hologram as a spatial modulation scheme is normalized to one, the output's peak height of the phase-only case has a value of 223. This means that the output signal of the phase-only case is 223 times stronger than that of the complex hologram case. Thus, in terms of system noise, the system with the phase-only hologram is robust about

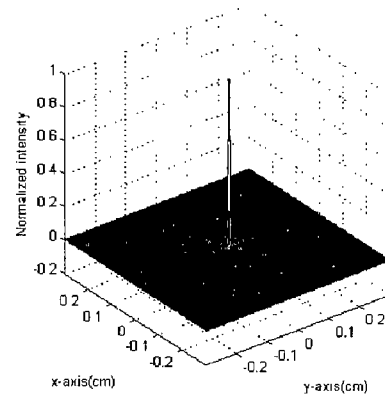


FIG. 11. Correlation output ( $0.4\text{ cm} \times 0.4\text{ cm}$ ) when the target object is matched with the reference object using phase-only hologram as a mask.

system noise. This result is directly related to the optical efficiency of the system. Because the phase-only hologram has 100 % optical efficiency, in other words, it does not block any light, we get a strong signal compared to the complex hologram modulation scheme. As a conclusion, we can deduce that the 3-D image matching system is very robust about additive noise in the input image regardless of the modulation schemes. The 3-D image matching system with a phase-only hologram is more robust than the complex hologram modulation scheme about system noise that is attributed to the detector and the optical components of the system itself.

## V. CONCLUSION

We have presented a phase-only modulation scheme to improve the optical efficiency of the 3-D holographic correlation technique. Optical efficiency is a critical issue for the 3-D holographic correlation because the robustness of the 3-D holographic matching system about the noise of the system highly depends on the optical efficiency. The modulation scheme with the phase-only hologram gives correlation results between the phase-only hologram of the reference object and the complex hologram of the target object. Since the phase-only hologram contains the emphasized version of whole 3-D lines, edges and other narrow events as well as depth information of the object, the correlation between the phase-only hologram and the complex hologram of the objects gives 3-D matching of the objects. We performed computer simulations with additional noise and without noise. Computer simulation results show that the system with a phase-only modulation scheme is robust about system noise. Because the phase-only hologram has 100 % optical efficiency, in other words, it does not block any light,

we get a strong signal compared to the complex hologram modulation scheme.

\*Corresponding author : takim@sejong.ac.kr.

### REFERENCES

- [1] Anil K. Jain and Patrick J. Flynn, *Three-Dimensional Object Recognition Systems* ( Elsevier Science Publishers, Amsterdam, The Netherlands, 1993).
- [2] J. Hofer-Alfeis and R. Bamler, Proc. SPIE 373, 77 (1981).
- [3] Y. B. Karasik, "Evaluation of three-dimensional convolutions by use of two- dimensional filtering." Appl. Opt. **36**, 7397 (1997).
- [4] J. Rosen, "Three-dimensional electro-optical correlation," J. Opt. Soc. Am. **A15**, 430 (1998).
- [5] T.-C. Poon and Taegeun Kim, Appl. Opt. **38**, 370 (1999).
- [6] Taegeun Kim and T.-C. Poon, Opt. Eng. **38**, 2176 (1999).
- [7] Taegeun Kim, T.-C. Poon , M. H. Wu, K. Shinoda, and Y. Suzuki, Optical Memory and Neural Networks, **8**, 139 (2000).
- [8] Taegeun Kim and T.-C. Poon, J. Opt. Soc. Am. **17**, 2520 (2000).
- [9] Taegeun Kim, Optical three-dimensional image matching using holographic information, Ph. D. Dissertation, Virginia Tech, 7 July, 2000.
- [10] J. L. Horner and Peter D. Gianino, Appl. Opt. **23**, 812 (1984).
- [11] J. L. Horner, Appl. Opt. **21**, 4511 (1982).
- [12] A. V. Oppenheim and J. S. Lim, Proc. IEEE 69, 529 (1981).